

# Simple setup for rapid testing of third-order nonlinear optical materials

Paul Horan, Werner Blau, Hugh Byrne, and Per Berglund

A relatively inexpensive and versatile degenerate four-wave mixing setup is described utilizing a nitrogen laser pumped dye laser. Samples can be screened rapidly, which is demonstrated with the example of a semiconductor doped glass having a nonlinear susceptibility  $\chi^{(3)} \sim 10^{-11}$ – $10^{-10}$  esu.

## I. Introduction

The field of nonlinear optics is concerned with the response of matter to high intensity light fields, such as are obtained with lasers. There is great interest in the subject, from the point of view of basic physics, and of possible applications. Nonlinear effects such as optical bistability and phase conjugation offer the possibility of all-optical signal processing, with the advantages of greater speed, integration with optical fiber technology, and the possibility of massively parallel computing.<sup>1</sup> Currently available materials do not match device requirements and so this field is dominated by the search for materials possessing a larger and/or faster nonlinear response.

To this end we have developed a simple measurement setup which allows routine testing of samples to be carried out rapidly (currently approximately one sample per day) and inexpensively. The method has been applied to molecular, polymeric, and colloidal materials as well as bulk and quantum-confined semiconductors and is illustrated here with the particular example of semiconductor doped glasses.

## II. Laser-Induced Grating Techniques

To study the nonlinear optical response of a particular material some method of altering the optical properties and investigating the changes is required. One such technique is a laser-induced grating (LIG).<sup>2</sup> Essentially, the procedure is to have two coherent light

beams overlap and thus interfere. This will produce a spatially modulated energy density in the interference region, with a period  $\Lambda$  where

$$\Lambda = \lambda/2 \sin(\theta/2), \quad (1)$$

where  $\theta$  is the angle between the writing beams and  $\lambda$  is the wavelength. The sample to be studied is placed in this region and with sufficient intensity a modulation of the material absorption  $\Delta\alpha$  and/or refractive index  $\Delta n$  will be produced [see Fig. 1(a)]. The spatial modulation of the optical parameters corresponds to an optical diffraction grating. The grating may be investigated by observing the diffraction of a probe beam, the diffraction efficiency depending on the degree of modulation induced. In absorbing samples an effective optical thickness  $d$ ,

$$d = (1 - T)/\alpha, \quad (2)$$

can be defined where  $\alpha$  is the absorption coefficient for a (physical) sample length  $l$  and  $T = \exp(-\alpha l)$  the sample transmission. For small absorption ( $\alpha \sim 0$ )  $d = l$  holds. In considering diffraction the separate regimes of thick and thin gratings must be identified. If the spacing of the created grating is the thickness as sample  $d$ , the Bragg condition must be satisfied, i.e., the angle of incidence must be equal to the angle of diffraction. In this thick regime essentially only one diffracted beam is observed. For a sufficiently thin sample the Bragg condition is relaxed. A grating is considered thin if the optical path difference of the diffracted beams is small compared to the wavelength. For near normal incidence this condition is satisfied if

$$d \ll 2\Lambda^2/\lambda. \quad (3)$$

In this case, diffraction will occur for any incident wave vector and a series of diffracted orders will be observed, as shown in Fig. 1(b).

The authors are with Trinity College, Department of Pure & Applied Physics, Dublin 2, Ireland.

Received 14 December 1988.

0003-6935/90/010031-06\$02.00/0.

© 1990 Optical Society of America.

The problem of Bragg diffraction from a thick holographic grating has been considered by Kogelnik.<sup>3</sup> For the general case of a mixed grating due to changes of absorption  $\Delta\alpha$  and of refractive index  $\Delta\eta$ , the diffraction efficiency is given by

$$I_1/I_0 = \exp(-2\alpha d) \left( \sin^2 \frac{\pi\Delta\eta d}{\lambda} + \sinh^2 \frac{\Delta\alpha d}{2} \right). \quad (4)$$

For a pure phase grating, i.e.,  $\Delta\alpha = 0$ , this simplifies<sup>4</sup> to

$$I_1/I_0 \sim (\pi\Delta\eta d/\lambda)^2. \quad (5)$$

For a pure amplitude grating ( $\Delta\eta = 0$ ), Eq. (4) simplifies to

$$I_1/I_0 \sim (\Delta\alpha d/2)^2. \quad (6)$$

These relationships hold for thin gratings also as the diffraction to higher orders is negligible when compared with the first order.

There are many possible geometries utilizing the LIG technique. The grating can be created by two beams and monitored with a third independent beam of the same or different wavelength. If the writing beams are pulsed, the decay of the grating can be studied by delaying the probe beam with respect to the creation of the grating or alternatively by using a cw probe. Very short (subpicosecond) time scale events can be monitored by creating a moving grating, which can be done by interfering two beams of different frequency (for overview see Ref. 2).

For sufficiently small absorption and thin grating conditions the two beams writing the grating will simultaneously self-diffract from the grating being created. In this case a series of diffraction orders will be observed to either side of the straight-through beams, spaced at approximately the angle between the writing beams. Although not as versatile as the three-beam techniques, the self-diffraction arrangement is much simpler to achieve experimentally. Also it is amenable to treatment using established degenerate four-wave mixing theory (see below).

An obvious disadvantage of the two-beam self-diffraction arrangement is the apparent lack of temporal resolution. Consider if the first-order diffracted beam is monitored while one pump is delayed with respect to the other by a time  $t$ . The system would be expected to act as an autocorrelator, with a response time equal to that of the pulses. However, by using phase modulated picosecond pulses (frequency width  $\Delta\nu$ ), more information may be gained. Phase modulated pulses are such that the coherence time of the pulse  $\tau_c$ , where  $\tau_c = 1/\Delta\nu$ , is much less than the pulse duration  $T$ . Self-diffraction with such pulses has been considered by Vasileva *et al.*<sup>5</sup> and the behavior is shown to depend on the ratio between the coherence time  $\tau_c$  and the relaxation time  $\tau_r$  of the excited state giving rise to the grating. For slow relaxation, i.e.,  $\tau_r \gg \tau_c$ , the diffracted energy should decay with a width  $\sim \tau_c$ . When the decay is fast, i.e.,  $\tau_r \ll \tau_c$ , a width equal to the pulse width  $T$  will be observed. Thus the resolution may be improved to equal the coherence time. However intermediate behavior is not resolved by this method.

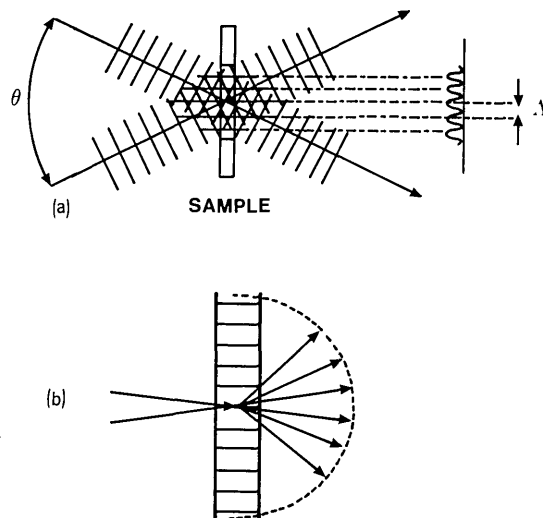


Fig. 1. (a) Producing a laser-induced grating and (b) diffraction from thin gratings.

### III. Degenerate Four-Wave Mixing and Self-Diffraction at a LIG

One well-known geometry used to study third-order processes is the so-called degenerate four-wave mixing (DFWM).<sup>6</sup> In this configuration, three different light fields  $E_1$ ,  $E_2$ , and  $E_3$  of the same frequency  $\omega$  (hence degenerate) are incident on a nonlinear medium. The three beams interact with the material to produce a fourth beam  $E_4$ . Generally  $E_1$  and  $E_2$  are known as the pump beams and are much stronger than the third beam known as the probe. DFWM can also be viewed as a LIG phenomenon. The grating is created by interference between  $E_1$  and  $E_3$ , and  $E_2$  diffracts off this grating to give  $E_4$ . Similarly the self-diffraction effect may be viewed as forward degenerate four-wave mixing. However, in this case the probe beam is equal to and collinear with one of the pump beams. For this geometry the magnitude of the third-order susceptibility can be calculated<sup>7</sup> as

$$\chi^{(3)} = \frac{8c^2 n^2 \epsilon_0 \alpha \sqrt{\eta}}{3\omega I_1 (1 - T)}, \quad (7)$$

where  $c$  is the speed of light,  $n$  is the linear refractive index,  $\alpha$  is the linear absorption,  $\omega$  is the frequency,  $I_1$  is the pump intensity, and  $T$  is the transmission at  $I_1$ . This allows the calculation of an effective third-order susceptibility from experimental measurements of the self-diffraction effect and knowledge of some physical parameters of the material. It should be noted that for constant  $\chi^{(3)}$  the diffraction efficiency depends quadratically, and thus the diffracted signal cubically, on the incident intensity  $I_1$ , as expected, for a third-order nonlinear process.

### IV. Experimental Technique for Laser-Induced Grating Studies

To investigate the nonlinear response of materials, laser-induced grating (LIG) measurements are usually carried out near the principal absorption maximum of

the material. This requires a tunable source of coherent light which was supplied by a nitrogen-pumped dye laser system (PRA LN1000 high pressure nitrogen laser and a PRA LN 107 high resolution dye laser<sup>8</sup>). Depending on the dye, the final output is a pulse of 40–100  $\mu\text{J}$ . The nitrogen pump pulse has a width of 800 ps, but due to thresholding effects in the dyes the LN107 has a rated output pulse length of 500 ps. Observation of the output with a vacuum photodiode and a fast storage oscilloscope yielded a pulse width of  $550 \pm 50$  ps. However, examination with a streak camera revealed some substructure in the pulse, which varied somewhat depending on the dye and tuning, and places an error of  $\pm 20\%$  on the determination of laser intensity.

The experimental setup is illustrated in Fig. 2. The lasers and all-optical components are on a  $4 \times 8$ -ft sheet of steel. This allows the use of magnetic mounts which provide a firm, yet versatile, mounting scheme. The output from the dye laser is collimated and brought around the table into a 50–50 beam splitter cube. To achieve temporal overlap of the pulses, a delay line is introduced on one arm; this is especially necessary because of the very short coherence length ( $\sim 4$  mm) of the pulses. The extra dispersion introduced by the prisms in the delay line is balanced by using two prisms to turn the second beam. The two collinear beams are brought to a focus and overlap by a 30- or 50-cm focal length lens. The beam waist is calculated using a series of calibrated pinholes and assuming a Gaussian beam profile, which is verified by an optical multichannel analyzer. To ensure that the beams overlap exactly in the sample, the turning prisms may be steered with micrometer positioning screws and adjusted to maximize the diffracted beam. When a material with a suitable nonlinear response is introduced into the overlap region, self-diffraction will occur. This may be observed by monitoring the beams on the opposite side of the sample. Two bright spots will be seen, corresponding to the straight-through beams. To either side, fainter spots at about the spacing between the pump beams appear corresponding to the diffracted beams. For highly nonlinear materials several orders may be observed. To illustrate this, the beams were imaged onto the linear CCD array of an optical multichannel analyzer system from B & M Spektronix. A typical image using a Schott semiconductor doped glass OG 530 is shown in Fig. 3, where the beams have been attenuated as indicated to lie within the dynamic range of the camera. The slight asymmetry results from the beams not being exactly equal in intensity.

To check that what is observed is truly due to diffraction rather than to some scattered light, the signal should disappear if either of the pump beams is blocked, i.e., the system should act as an optical AND gate. In practice, when measuring the magnitude of the diffracted beam the signal obtained with the nearer pump beams blocked was also measured and subtracted from the diffracted signal. This removes the component due to background scatter and it also

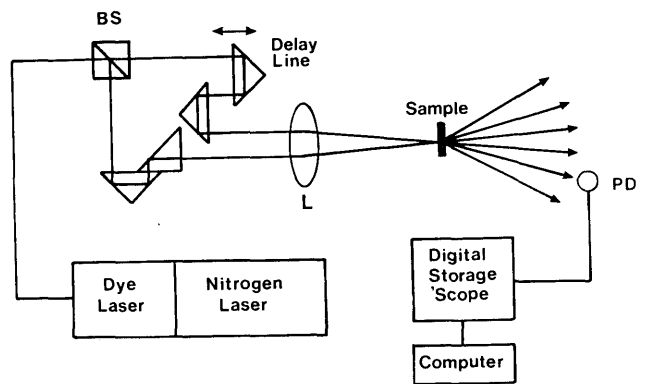


Fig. 2. Experimental arrangement for observing self-diffraction from a laser-induced grating.

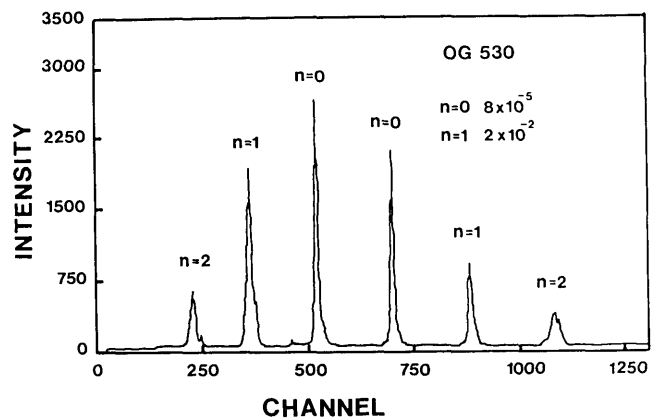


Fig. 3. CCD camera/OMA image of the diffracted orders. The zeroth and first orders are attenuated as noted.

ensures that only a transient grating is measured. Permanent gratings can be written by physical damage to a material or by other photochemical effects such as the darkening phenomenon. This precaution greatly improves result reliability.

For normal operation the first diffracted order was aligned through a narrow pinhole to reduce scattered light and then incident on a large area silicon photodiode. Suitable neutral density filters were used to avoid saturating the photodiode response. The output voltage pulse is proportional to the input energy and is calibrated using a Gentec ED-100A fast-response pyroelectric detector. The voltage was measured using a Vuko VKS 220-16 digital storage oscilloscope. For ease of operation the scope had been interfaced with a BBC microcomputer. This allowed a specified number of pulses to be measured and averaged, the results then being displayed or stored on disk. The system can handle two channels allowing the simultaneous monitoring of the input and diffracted energies.

## V. Experimental Results from LIG Measurements

The above apparatus was used to study self-diffraction in Schott  $\text{CdS}_x\text{Se}_{1-x}$  doped glasses. An earlier LIG study of these glasses by Eichler *et al.*<sup>9</sup> had reported saturable absorption. On monitoring the diffracted intensity with increasing input intensity at a fixed (ruby) wavelength, they observed the expected cubic behavior at low intensities, with a less than cubic dependence at higher intensities, indicative of absorption saturation. Similar measurements were carried out, but showed only the cubic behavior predicted by Eq. (7), i.e., the intensities available were insufficient to achieve appreciable saturation. Typical results are shown in Fig. 4.

In an effort to understand the nonlinear mechanism operating wavelength-resolved measurements were carried out across the bandgap. On measuring the diffraction efficiency, a maximum is usually observed for a sample transmission of 20–30%. This behavior may be explained qualitatively as a trade-off between increasing coupling of the pump beams vs increasing absorption of the signal, giving some maximum. Results are shown in Fig. 5. Subtraction of the signal obtained with one pump beam blocked, as described in the previous section, ensures that only the transient grating is measured, removing any contribution from any permanent grating which may be created by the darkening effect observed in those glasses due to long-lived carrier trapping effects.<sup>10</sup>

Having measured the diffraction efficiency, Eq. (7) was used to calculate an effective third-order susceptibility. The results of these calculations, together with the absorption spectrum for the OG 530 glass, are illustrated in Fig. 6. The third-order susceptibility is of the order observed by other workers.<sup>9–12</sup> The major point to note is the linear relation between absorption and  $\chi^{(3)}$ . Similar dependence on absorption has also been observed by Roussignol *et al.*<sup>10</sup> The actual measured susceptibilities of  $10^{-10}$ – $10^{-11}$  esu are not very large for semiconductor materials. It must be noted however that the glass is only doped at a volume factor of  $10^{-3}$ – $10^{-4}$ , so the effective susceptibility per active volume is appreciable.

The initial report on DFWM in glasses by Jain and Lind<sup>11</sup> suggested that the nonlinearity was due to plasma generation. They achieved reasonable numerical agreement for  $\chi^{(3)}$  at a fixed wavelength (532 nm), but the plasma model predicts a strong resonance at the bandgap which is not observed. The simple two-level saturation model, see, e.g., Caro and Gower,<sup>7</sup> is also excluded, as it predicts  $\chi^{(3)} \sim (\alpha\lambda)^2$ . Band filling is a likely effect and has been suggested by Roussignol *et al.*<sup>10</sup> and Olbright *et al.*<sup>12</sup> Band filling arises from relaxation of free carriers to the band extrema before recombination and thus blocking these transitions. That the carriers relax and fill all the lowest lying states up to some level is a result of applying Fermi-

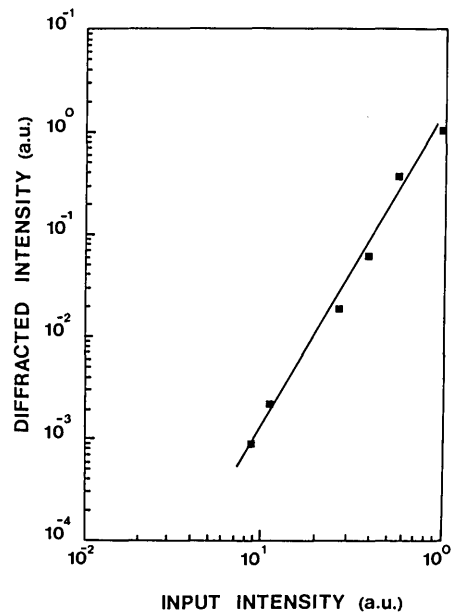


Fig. 4. Typical logarithmic plot of diffracted intensity vs incident intensity. The fit is to a slope of 3; sample OG 530; wavelength 521 nm.

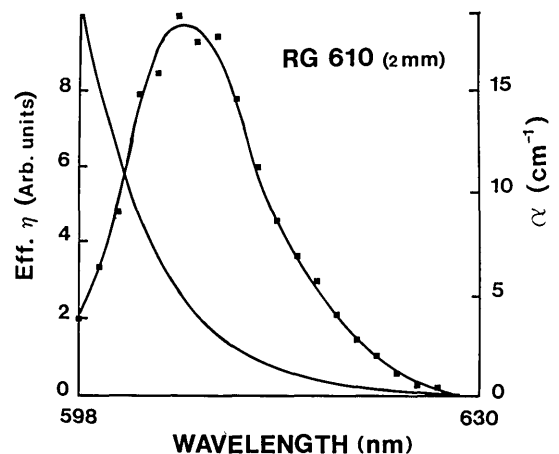


Fig. 5. Measured diffraction efficiency for Schott glass RG 610.

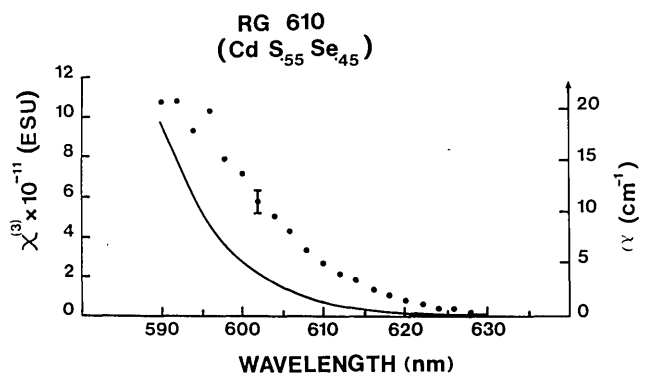


Fig. 6. Calculated third-order nonlinear susceptibility (solid circles) and linear absorption coefficients (curves) for Schott glass RG 610.

Dirac statistics. An analysis of this effect<sup>13</sup> predicts that

$$\chi^{(3)} \approx \alpha(\omega)/(\omega_g - \omega). \quad (8)$$

This is not in agreement with results. Operating close to the band edge, as has been done, means that the detuning factor in Eq. (8) should be significant, but this is not observed.

Band filling has also been considered with nondegenerate Boltzmann statistics.<sup>14</sup> In this case  $\chi^{(3)}$  is essentially dependent on absorption only. This model has been discussed by Roussignol *et al.*,<sup>10</sup> and it can also account for their saturation observations. They argue that Boltzmann statistics are applicable in this case, working at room temperature and in the absorption tail. In agreement with the data presented here, this model does provide a reasonable explanation for the primary nonlinear mechanism in these glasses, where essentially bulk behavior is to be expected.

Delaying one pulse with respect to the other does yield some information for phase modulated pulses, as outlined in Sec. II. Phase modulated means that the coherence time of the pulse  $\tau_c$  is much shorter than the pulse length  $T$ . The LN1000/LN107 combination produces pulses of 500 ps, but the narrow spectral bandwidth of  $<0.5 \text{ \AA}$  corresponds to a coherence time  $<17 \text{ ps}$  at 500-nm wavelength, so these pulses well satisfy the definition of being phase modulated in the visible region. Results for the glass RG 610 are shown in Fig. 7. The FWHM corresponds to 12 ps, which can be taken to be the coherence time. This indicates that the relaxation time of the principal mechanism giving rise to the grating is long compared with 12 ps. The sidelobes observed are due to a small secondary pulse along with the main one, as also suggested by streak camera readings. The lower limit of 12 ps is reasonable at these intensities. In fact, the wide discrepancy in reported relaxation times, from 10 ps (Ref. 15) to 72  $\mu\text{s}$ ,<sup>16</sup> indicates the problems that exist with these materials. Recombination of an excited population of carriers can be expected to be some combination of direct recombination, surface recombination, followed by decay of trapped carriers. Measured recombination times have been observed by several groups to be strongly intensity dependent. As an example, in the glass RG 610 the measured grating decay constant went from  $\sim 10$  to 2 ps for intensities of 1 and 5  $\text{GW}/\text{cm}^2$ , using 0.5-ps pulses. The mechanism of this intensity dependence is unclear, although Auger recombination has been suggested.<sup>17</sup> The situation is further complicated by the knowledge that the time scale is altered by the photochemical darkening effect.<sup>10</sup> For fresh, undarkened samples, a slow decay of a grating is observed on the scale of tens of nanoseconds. However, working with a darkened area of the same glasses, a fast component of 50–100 ps is reported. A similar variation is seen in the temporal decay of photoluminescence from fresh and darkened samples. A full explanation of the temporal evolution of an excited state population must still be found.

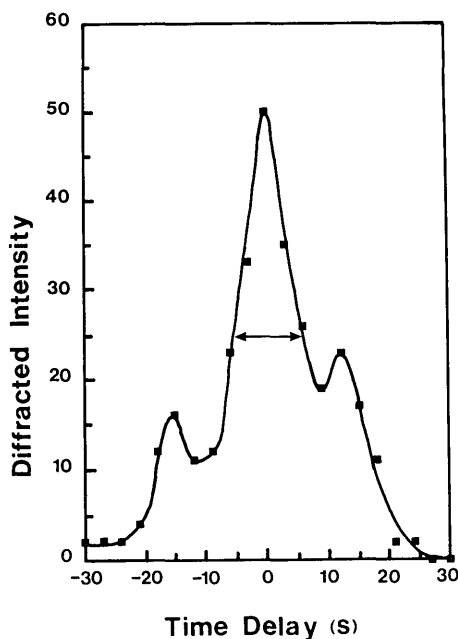


Fig. 7. Diffracted intensity vs delay for Schott glass RG 610; wavelength 600 nm.

## VI. Conclusions

These results demonstrate the versatility and usefulness of the experimental setup described. Furthermore, they elucidate some properties of the semiconductor doped glass: The first point that should be made is that the commercially available semiconductor doped glasses are not quantum confined systems. The observed behavior can be explained in terms of bulk semiconductor properties, albeit modified by the large surface-to-volume ratio of such small particles. They possess a large nonlinear optical response when the small volume ratio is considered, operating on a picosecond scale if suitably treated. The principal nonlinear mechanism appears to be band filling but greatly modified by the secondary darkening effect and the large surface area available. The detailed understanding of the recombination process is not yet clear.

As inexpensive and readily available nonlinear optical materials semiconductor doped glasses will continue to be of interest. The wide operating spectrum makes them very versatile. They are excellent for aligning a nonlinear optical experiment. Applications such as the fabrication of waveguides are well advanced<sup>18</sup> and will ensure continued study of these most interesting materials for some time to come.

Part of this work was supported by the Commission of the European Communities under the RACE program and also by EOLAS, the Irish Science & Technology Agency.

P. Berglund is a visiting student from Lund University, Sweden.

## References

1. C. Flytzanis and J. L. Oudar, Eds., *Nonlinear Optics: Materials and Devices* (Springer-Verlag, Berlin, 1985).
2. H. J. Eichler, P. Gunter, and D. W. Pohl, *Laser Induced Dynamic Gratings* (Springer-Verlag, Berlin, 1986).
3. H. Kogelnik, "Coupled Wave Theory for Thick Hologram Gratings," *Bell Syst. Tech. J.* **48**, 2909-2947 (1969).
4. H. J. Eichler, "Laser-Induced Grating Phenomena," *Opt. Acta* **24**, 631-642 (1977).
5. M. A. Vasileva, J. Vishakas, V. Kalbelka, and A. V. Masalov, "Measurement of Relaxation Times by Phase Modulated Ultrashort Light Pulses," *Opt. Commun.* **53**, 412-416 (1985).
6. R. A. Fisher, Ed., *Optical Phase Conjugation* (Academic, Orlando, 1984).
7. R. C. Caro and M. C. Gower, "Phase Conjugation by Degenerate Four-Wave Mixing in Absorbing Media," *IEEE J. Quantum Electron.* **QE-18**, 1375-1380 (1982).
8. PRA International, 45 Meg Drive, London, Ontario, Canada.
9. H. J. Eichler, G. Enterlein, P. Glozbach, J. Munschau, and H. Stahl, "Power Requirements and Resolution of Real-Time Holograms in Saturable Absorbers and Absorbing Liquids," *Appl. Opt.* **11**, 372-375 (1972).
10. P. Roussignol, D. Ricard, J. Lukasik, and C. Flytzanis, "New Results on Optical Phase Conjugation in Semiconductor-Doped Glasses," *J. Opt. Soc. Am. B* **4**, 5-13 (1987).
11. R. K. Jain and R. C. Lind, "Degenerate Four-Wave Mixing in Semiconductor-Doped Glasses," *J. Opt. Soc. Am.* **73**, 647-653 (1983).
12. G. R. Olbright, N. Peyghambarian, S. W. Koch, and L. Banyai, "Optical Nonlinearities of Glasses Doped with Semiconductor Microcrystallites," *Opt. Lett.* **12**, 413-415 (1987).
13. B. S. Wherrett and N. A. Higgins, "Theory of Nonlinear Refraction Near the Band Edge of a Semiconductor," *Proc. R. Soc. London Ser. A* **379**, 67-90 (1982).
14. D. A. B. Miller, C. T. Seaton, M. E. Prise, and S. D. Smith, "Band-Gap-Resonant Nonlinear Refraction in III-V Semiconductors," *Phys. Rev. Lett.* **47**, 197-200 (1981).
15. D. Cotter, "Time-Resolved Picosecond Optical Nonlinearity in Semiconductor-Doped Glasses," *Electron. Lett.* **22**, 693-694 (1986).
16. J. T. Remillard and D. G. Steel, "Narrow Nonlinear-Optical Resonances in CdS<sub>2</sub>-Doped Glass," *Opt. Lett.* **13**, 30-32 (1988).
17. F. de Rougement, R. Frey, P. Roussignol, D. Ricard, and C. Flytzanis, "Evidence of Strong Auger Recombination in Semiconductor-Doped Glasses" *Appl. Phys. Lett.* **50**, 1619-1621 (1987).
18. H. Jerominek, M. Pigeon, S. Patela, Z. Jabukczyk, C. Delisle, and R. Tremblay, "CdS Microcrystallites-Doped Thin-Film Glass," *J. Appl. Phys.* **63**, 957-959 (1988).